

Domain size effects in a uniaxial ferroelectric relaxor system: The case of $\text{Sr}_x\text{Ba}_{1-x}\text{Nb}_2\text{O}_6$

Uwe Voelker, Urs Heine, Christoph Gödecker, and Klaus Betzler^{a)}

Fachbereich Physik, Universität Osnabrück, Barbarastrasse 7, D-49069 Osnabrück, Germany

(Received 3 September 2007; accepted 16 October 2007; published online 13 December 2007)

We present investigations of the domain dynamics and of the evolution of the critical exponent β in a ferroelectric relaxor system, exemplarily in the up-to-date controversial strontium barium niobate (SBN). k -space spectroscopy at the phase-transition and when applying an electric field reveals a size-dependent response of the domains. This is supported by pyroelectric measurements that show, by analysis in terms of criticality, the critical exponent β is not only dependent on the level of poling but also on the manner in which the poling was achieved. It must be concluded that the crystals undergo a phase transition not—as commonly assumed—in a uniform way with homogeneous polarization throughout the crystal. Instead they behave as a set of more or less independent domains with size-dependent stability. Therefore, one should be very careful with critical exponents—especially those derived from experiments that explicitly or implicitly—assume a uniform polarization behavior. © 2007 American Institute of Physics. [DOI: 10.1063/1.2821754]

I. INTRODUCTION

The uniaxial relaxor ferroelectric strontium barium niobate [$\text{Sr}_x\text{Ba}_{1-x}\text{Nb}_2\text{O}_6$, (SBN)] shows a phase transition, which is extended over a broad temperature region. Thus, the transition cannot be characterized by a sharp Curie temperature T_C ; instead a “Curie region” is defined within which the order parameter, the spontaneous polarization P , approaches zero. Usually the inflection point T_i in the temperature dependence of P is chosen as the characteristic temperature for the phase transition. In order to classify the type of the relaxor phase transition with regard to criticality, various groups tried to determine the “critical exponents” for the phase transition, especially the critical exponent β , which governs the behavior of P near T_C according to

$$P(T) = P_o \left(1 - \frac{T}{T_c}\right)^\beta \quad \text{for } T \lesssim T_c. \quad (1)$$

Chen *et al.* conducted “thermal self-focusing” experiments, which yield a critical exponent $\beta=0.32-0.34$ (Ref. 1). By measuring the linear birefringence as a function of the temperature, Lehnen *et al.* calculated $\beta=0.31\pm 0.01$ (Ref. 2). One year later, Blinc *et al.* performed ^{93}Nb NMR measurements on SBN, which contrastingly yield $\beta=0.15\pm 0.03$ by fitting Eq. (1) to their data.³ By applying the same technique, Kleemann *et al.* found a critical exponent $\beta=0.14\pm 0.03$ [and, additionally, $\gamma(350 \text{ K})=1.85$] (Ref. 4). They claimed a ferroic “three-dimensional (3D) random field Ising model” to be materialized in SBN, since this parameter matches the corresponding numerically simulated value of $\beta=0.017\pm 0.005$ (Ref. 5) better than the value calculated for the 3D random bond Ising model, $\beta=0.349$ (Ref. 6). In 2006, β values achieved by second-harmonic measurements were published with $\beta\approx 0.10\pm 0.03$ (Ref. 7) and $\beta\approx 0.13\pm 0.02$, which is approximately equal to $1/8$ (Ref. 8). In the latter

publication, the authors claim the critical exponents to be “two-dimensional Ising-model-like.” Granzow *et al.* go even beyond the listed publications and investigate the evolution of the critical exponent β as a function of the poling state of the SBN crystal.⁹ Thus, they fit Eq. (1) with $0.13\leq\beta\leq 0.30$ to data for SBN:Ce achieved by pyroelectric measurements starting at different initial polarizations from 100% down to 0.8% of the saturation value. This finding is interpreted as a change from 3D-Ising to random field Ising-model criticality in SBN.

In the present article, we report on measurements of the ferroelectric domain structuring in SBN in the vicinity of the Curie region and at room temperature under external electric fields. For the evolution of β for different initial polarization states of the crystal, i.e., β as a function of $P(T=300 \text{ K})$, we get results that contradict—or at least expand—former ones and show that it is rather problematic to define a unique β for the whole crystal.

II. EXPERIMENTAL DETAILS

For the investigation of the domain structuring in SBN, we applied “ k -space spectroscopy” to the crystal. This technique is based on (random) quasi-phase-matching for optical second-harmonic generation (SHG) described by the momentum condition

$$\mathbf{k}_2 = 2\mathbf{k}_1 + \mathbf{k}_g. \quad (2)$$

Here, \mathbf{k}_1 and \mathbf{k}_2 denote the wave vectors of fundamental and harmonic waves, respectively. The additional momentum contribution \mathbf{k}_g required is provided by the Fourier representation of the domain structure. The angular and density distribution of \mathbf{k}_g is reflected in the angular distribution and intensity of the second-harmonic light. Varying the directions of \mathbf{k}_1 and \mathbf{k}_2 facilitates the inspection of the \mathbf{k}_g distribution, thus the domain size distribution.⁷

Our measurements of SBN show an expressed anisotropy of the \mathbf{k}_g distribution—a detectable second-harmonic

^{a)}Electronic mail: Klaus.Betzler@uos.de

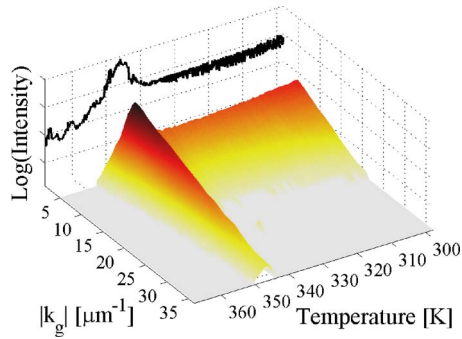


FIG. 1. (Color online) k -space spectra at the relaxor phase transition of SBN: angular (i.e., $|\mathbf{k}_g|$) distribution of the harmonic intensity as a function of temperature. The data gap between $|\mathbf{k}_g|=1.5$ and $5 \mu\text{m}^{-1}$ is due to the restricted dynamic range of the measuring systems.

intensity is only found in the plane perpendicular to the c axis of the crystals. This is consistent with the agreed model that SBN consists of “needlelike” domains,¹⁰ which are extended in the c -axis direction but small perpendicular to it.¹¹ Furthermore, the intensity pattern does not change when the crystals are rotated around c , which indicates that there is no preferred direction perpendicular to the β axis. These two fundamental features are found to be independent of a variation of other parameters. Therefore we could restrict our measurements on a planar configuration where the angle α between \mathbf{k}_1 and \mathbf{k}_2 was varied, yielding

$$|\mathbf{k}_g| = (4|\mathbf{k}_1|^2 + |\mathbf{k}_2|^2 - 4|\mathbf{k}_1||\mathbf{k}_2|\cos \alpha)^{1/2}. \quad (3)$$

For our measurements, we used SBN crystals grown from the congruently melting composition (strontium fraction $x=0.61$). Both undoped and slightly europium-doped crystals (Eu content 0.12 mol % in the crystal) were investigated in the following denoted as SBN61 and SBN61:Eu, respectively. Except for a shift in T_i (350 K for the undoped, 345 K for the doped samples), no difference in the behavior was found, i.e., slight doping does not cause any peculiarities.

Three types of measurements were performed:

- k -space spectroscopy during the heating cycle of field-cooled (FC) samples. Before the measurements, the samples were heated to a temperature of 425 K, well above the phase transition, then slowly cooled down to room temperature under an applied electric field of 350 V/mm parallel to the crystallographic c axis.
- Pyroelectric measurements. The sample was mounted on a temperature-controlled peltier stack with a temperature stability of 0.1 K applying a heating rate of 0.0125 K s^{-1} . The c faces were covered by conductive silver. The measurement of the surface charge was performed by a Keithley 6514 electrometer.
- k -space spectroscopy while applying an electric field to unpoled samples at room temperature.

III. RESULTS AND DISCUSSION

A. k spectra at the phase transition

Figure 1 shows the k spectra of an SBN61:Eu crystal

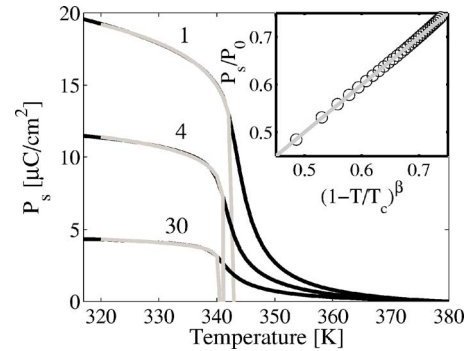


FIG. 2. (Color online) Polarization as a function of temperature for the first, fourth, and thirtieth measuring cycle. The gray lines indicate a fit of Eq. (1) to the according data. The inset shows a plot of the normalized polarization P/P_0 as a function of the reduced temperature $(1-T/T_c)^\beta$ to the power β (circles), including a line through origin with a slope of 1 (gray).

achieved by k -space spectroscopy (type A measurement). The second-harmonic intensity is plotted as a function of $|\mathbf{k}_g|$ and of the crystal temperature. The solid black line in Fig. 1 represents data measured at the lowest accessible $|\mathbf{k}_g| \approx 1.5 \mu\text{m}^{-1}$. For temperatures spanning from room temperature up to the Curie region near 340 K, substantial intensities are only found near $|\mathbf{k}_g|=0$. This indicates that the crystal is in a poled state, i.e., a “single domain state” throughout this range. Within the Curie region, an expressed increase in the intensity for larger $|\mathbf{k}_g|$ -values is found, indicating the disintegration of the single domain state into smaller-structured domains.⁷ Thus, k -space spectroscopy shows that—starting from a low-temperature homogeneously poled state—an inhomogeneous state is reached in the temperature range of the Curie region. This state is characterized by a broad distribution of structural sizes, stabilized by crystal inhomogeneities (also denoted as “random fields”). It should be noted that switching from heating to cooling at any arbitrarily chosen temperature in this region does not restore the previous poled state. Instead, the broad $|\mathbf{k}_g|$ distribution persists to lower temperatures. Different states at identical temperatures, however, indicate that we are not in thermodynamic equilibrium.

B. Repoling behavior

To clarify this point in more detail, we investigated the repoling behavior of field-cooled SBN without an applied electric field. SBN is known to show a strong repoling characteristic,¹² which is assumed to be due to random electric fields in SBN.¹³ These random fields are supposed to be stabilized by trapped charge carriers, trapped in accordance with the electric field applied during the poling procedure. Heating field-cooled crystals without an applied electric field to temperatures not too far beyond the Curie region and cooling back leads to polarization that is distinctly smaller than the previous one. We studied this effect by pyroelectric measurements (“type B measurements”) on originally homogeneously poled crystals, determining the polarization and the critical exponent β . The temperature was cycled between 300 and 380 K.

In Fig. 2, the solid black lines show the polarization P as a function of temperature for the first, fourth, and thirtieth measuring cycle. The gray lines are fits of Eq. (1) to the

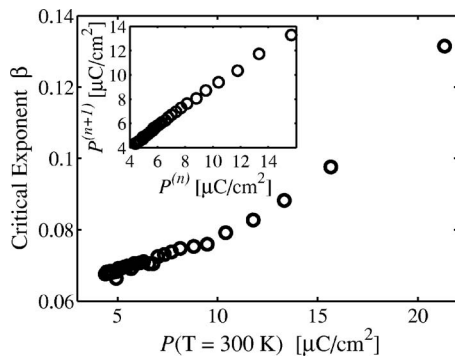


FIG. 3. Critical exponent β vs initial polarization of the crystal at the start of each loop, achieved by repoling. β was obtained by fitting Eq. (1) to the experimental data of the pyroelectric measurements. In the inset the polarization $P^{(n+1)}$ after every cycle is plotted as a function of the respective starting polarization $P^{(n)}$, each at $T=300$ K.

experimental data, respectively. It can be seen that the evolution of the polarization with temperature changes its shape depending on the initial polarization. The inset is a plot of the normalized polarization P/P_0 versus reduced temperature $(1-T/T_c)$ to the power β for the first measuring cycle. The gray line in turn is a line through the origin with a slope of 1. As expected, the data in the inset match the straight line quite well.

The repoling characteristic of an SBN61:Eu crystal is illustrated in the inset in Fig. 3. The polarization at the end of each measuring loop is plotted as a function of the respective start polarization (both at 300 K). The results of a sequence of 30 loops show a linear dependence with a slope of 0.81 ($P^{(n+1)}=0.81P^{(n)}$). As shown exemplarily for three curves in Fig. 2, we determined the critical exponent β as a function of the respective initial polarization $P(T=300$ K) from a fit of Eq. (1) to our data. The results are plotted in Fig. 3. The critical exponent β decreases from 0.13 to 0.065 for polarizations decreasing from 22 to 4 $\mu\text{C}/\text{cm}^2$.

The fact that β decreases by a factor of ≈ 2 with decreasing polarization is in fundamental contradiction to the results presented by Granzow *et al.*⁹ who found that β increases with decreasing polarization. The main difference between the two experiments is the way in which the reduced polarization was achieved. In contrast to our measurements, Granzow *et al.* poled the samples at room temperature partially, applying appropriately reduced electric fields.

From the different β values for identical values of the saturation polarization it follows that at least one, or presumably both, of the polarization states do not represent crystals in thermodynamic equilibrium. Different types of domain structures seem to be favored by the different experimental treatments. Obviously through our treatment preferably energetically stable structures persist in the cycling, whereas poling with reduced fields at room temperature prefers easily switchable structures. In both cases the polarization P is not homogeneous through the crystal, thus P should not be used as a global-order parameter when dealing with (partially) poled crystals.

C. k spectra due to external electric fields

Ferroelectric crystals are *inter alia* defined by the possibility to switch the direction of the spontaneous polarization

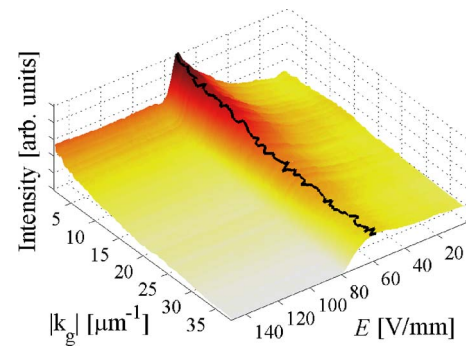


FIG. 4. (Color online) Plot of the second-harmonic intensity as a function of $|\mathbf{k}_g|$ and of the external electric field E applied. The black line indicates the positions $E^{(M)}$ of the intensity peaks.

by applying an electric field. This results in a typical ferroelectric hysteresis curve as measured for SBN, e.g., in Ref. 14. For an unpoled ferroelectric, an increasing electric field leads to the initial polarization curve. To account for size effects during the application of an electric field, we measured the k -space spectrum during the initial polarization of SBN at room temperature (“type C measurement”). Prior to the measurements, the crystals were annealed for 4 h at 670 K to erase any spurious polarization. Figure 4 shows the second-harmonic intensity as a function of $|\mathbf{k}_g|$ and of the external electric field E for an undoped sample (SBN61).

As already described in Ref. 7 the zero-field situation is characterized by a constant intensity distribution for all $|\mathbf{k}_g|$ accessible. By increasing the electric field from zero to higher values, a $|\mathbf{k}_g|$ -dependent increase in the second-harmonic signal is observed, indicating an accordant increase in the density of the correspondingly sized structures. At certain values $E^{(M)}$, connected by the black line in Fig. 4, the second-harmonic intensity peaks, followed by a decrease at a further increased field. The high-field situation is characterized by second-harmonic intensities, i.e. $|\mathbf{k}_g|$ densities, which are considerably lower than the zero-field ones at high $|\mathbf{k}_g|$, albeit considerably higher at very low $|\mathbf{k}_g|$ values.

Figure 5 shows a closer analysis of the data presented in Fig. 4. The electric field at which the second-harmonic intensity peaks, $E^{(M)}$, is plotted as a function of $|\mathbf{k}_g|$. The gray line is a linear fit to the data represented by the circles.

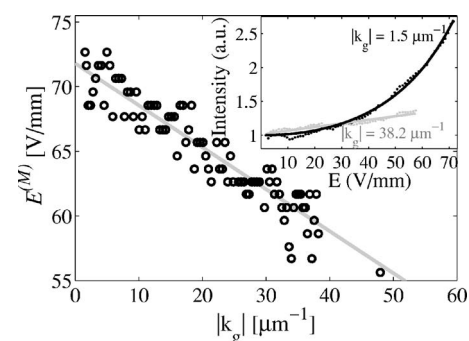


FIG. 5. Plot of the field $E^{(M)}$, where the second-harmonic intensity peaks (see Fig. 4), as a function of $|\mathbf{k}_g|$. Circles represent experimental data; the gray line is a linear fit to the data. The inset shows the slope of intensity to the peak for $|\mathbf{k}_g|=1.5$ μm^{-1} (black dots) and $|\mathbf{k}_g|=38.2$ μm^{-1} (gray dots).

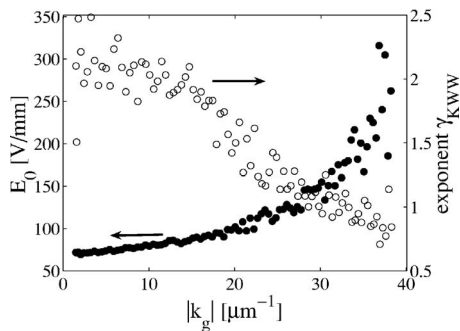


FIG. 6. Plot of the parameters from a fit of Eq. (4) to the data plotted in Fig. 4 as a function of $|\mathbf{k}_g|$.

The inset in Fig. 5 shows the second-harmonic intensity from zero field up to the peak as a function of external electric field for two $|\mathbf{k}_g|$ values. The lines denote fits of a stretched exponential function according to Kohlrausch, Williams, and Watts [(KWW) function],

$$I = \exp\left[\left(\frac{E}{E_0}\right)^{\gamma_{\text{KWW}}}\right] \quad (4)$$

to the data. It can be seen that this function describes the data well in both depicted cases. To investigate the $|\mathbf{k}_g|$ dependency of the second-harmonic intensity as a function of E numerically, we fitted Eq. (4) to the data presented in Fig. 4. As can be seen in Fig. 6, both parameters E_0 and γ_{KWW} show a strong dependency on the grating vector $|\mathbf{k}_g|$. The denominator E_0 (black dots) seems to increase in an exponential manner with increasing $|\mathbf{k}_g|$. Simultaneously, the stretching exponent γ_{KWW} decreases nearly linearly. Thus, the curvature of second-harmonic intensity as a function of E is quite straight and flat for large $|\mathbf{k}_g|$, while it gets steeper and curved with decreasing $|\mathbf{k}_g|$.

The poling of a crystal, detectable by surface charge measurements, is the macroscopic expression of domain switching on a microscopic scale. This switching is forced by the applied electric field E , as demonstrated by real time observation using electro-optic imaging microscopy.^{15,16} In addition to the findings in these publications, our measurements show that domain switching does not happen in a unique way for all structural sizes. Instead, the size dependence of the peak field $E^{(M)}$ in the k -space spectra must be explained as follows: By increasing the external field, the structures favored by the field grow larger—at the expense of the density of smaller domains. Thus, domain sizes shift from small to large scale. Connected with this shift, a density maximum traverses through the $|\mathbf{k}_g|$ - E plane, showing up as an intensity maximum in the k spectra. This maximum is at a lower field for small domains and at higher one for large domains (Fig. 5). According to this, it must be concluded that smaller structures are aligned by lower electric fields, rather than larger ones, in the relaxor ferroelectric SBN. Furthermore, it is numerically evident that the dynamics of domain formation is dependent on their size. Since the second-harmonic intensity's shape develops from flat to steep for smaller $|\mathbf{k}_g|$ values (see Figs. 4 and 6), we have to assume that their density distribution develops in the same manner. Thus, a kind of avalanche effect must be assumed in unpoled

SBN, regarding the density of domain sizes as a function of electric field. The growth of large domains should be accompanied by a discreation of smaller ones, or in other terms, by domain wall motions transferring small domains into larger ones, as evidenced by the second-harmonic peak distribution plotted in Fig. 5. The velocity of the domain wall motion depends on the local electric field, which is in turn dependent on the applied external electric field and the neighboring domains.

Our results further show that SBN exhibits a broad distribution of structural sizes. The immediate consequence of this is a spatially varying polarization in such ferroelectrics—at least during the poling process and in all so-called partially poled states.

IV. CONCLUSION

Our findings strongly affect all integral methods to characterize the ferroelectric behavior and especially the phase transition of SBN. Nonintegral methods, on the other hand, are affected by the size-dependent stability of the domains. This may be one reason for the different values of the critical exponent β found by different techniques.

In summary, we investigated the behavior of domains in the ferroelectric relaxor system SBN using k -space spectroscopy as nonintegral and pyroelectric measurements as integral techniques. The following results and conclusions have been drawn:

- (1) Homogeneously poled crystals do not undergo the ferroelectric-paraelectric phase transition in a unique way.
- (2) Neither poled nor partially poled crystals are in a thermodynamic equilibrium state.
- (3) The polarization of partially poled and unpoled crystals varies spatially.
- (4) The structural stability depends on the typical structural size.
- (5) The critical exponents derived depend both on the technique used for the preparation of the sample state and on the type of the measurement.
- (6) The switching dynamics of domains in an unpoled SBN crystal are dependent on the respective domain sizes.

The so-called relaxor behavior of crystals such as SBN thus must be referred to spatial inhomogeneities caused by the crystal structure itself and/or by the defect distribution. These inhomogeneities reveal a distribution of the energetic stability of differently sized domain structures. As shown by our experimental results, this stability distribution shows up in a field-dependent response, a broad Curie region, and critical exponents arbitrarily tunable by the experimental procedures used.

Our results strongly support the criticism issued by Chao *et al.*¹⁷ and Scott,¹⁸ who argue that critical exponents in such systems cannot be derived due to the lack of thermal equilibrium. The phase transition in such systems is not a unique one. Instead a domain size-dependent phase transition on a microscopic scale (Fig. 1) and a preparation- and approach-dependent phase transition on a macroscopic scale (Fig. 3)

are characteristic for such materials. The distinct domain size dependence may be the fundamental reason for the failure of most scaling attempts in these materials (for a review on this problem, see e.g., Refs. 18 and 19).

ACKNOWLEDGMENTS

The financial support from the Deutsche Forschungsgemeinschaft within the Graduiertenkolleg GRK 695 is gratefully acknowledged. The authors thank Dr. R. Pankrath for supplying the samples.

¹T. Chen, S. J. Sheih, J. F. Scott, and H. C. Chen, *Ferroelectrics* **120**, 115 (1991).

²P. Lehnen, W. Kleemann, T. Woike, and R. Pankrath, *Eur. Phys. J. B* **14**, 633 (2000).

³R. Blinc, A. Gregorovic, B. Zalar, R. Pirc, J. Seliger, W. Kleemann, S. G. Lushnikov, and R. Pankrath, *Phys. Rev. B* **64**, 134109 (2001).

⁴W. Kleemann, J. Dec, P. Lehnen, R. Blinc, B. Zalar, and R. Pankrath, *Europhys. Lett.* **57**, 14 (2002).

⁵A. A. Middleton and D. S. Fisher, *Phys. Rev. B* **65**, 134411 (2002).

⁶G. Jug, *Phys. Rev. B* **27**, 609 (1983).

⁷U. Voelker and K. Betzler, *Phys. Rev. B* **74**, 132104 (2006).

⁸W. Kleemann, J. Dec, V. V. Shvartsman, Z. Kutnjak, and T. Braun, *Phys. Rev. Lett.* **97**, 065702 (2006).

⁹T. Granzow, T. Woike, M. Wöhlecke, M. Imlau, and W. Kleemann, *Phys. Rev. Lett.* **92**, 065701 (2004).

¹⁰D. Viehland, Z. Xu, and W.-H. Huang, *Philos. Mag. A* **71**, 205 (1995).

¹¹P. Lehnen, W. Kleemann, T. Woike, and R. Pankrath, *Phys. Rev. B* **64**, 224109 (2001).

¹²T. Granzow, U. Dorfler, T. Woike, M. Wöhlecke, R. Pankrath, M. Imlau, and W. Kleemann, *Appl. Phys. Lett.* **80**, 470 (2002).

¹³T. Granzow, U. Dorfler, T. Woike, M. Wöhlecke, R. Pankrath, M. Imlau, and W. Kleemann, *Europhys. Lett.* **57**, 597 (2002).

¹⁴R. Maciolek and S. Liu, *J. Electron. Mater.* **2**, 191 (1973).

¹⁵L. Tian, D. A. Scrymgeour, and V. Gopalan, *J. Appl. Phys.* **97**, 114111 (2005).

¹⁶C. Huang, A. Bhalla, and R. Guo, *Appl. Phys. Lett.* **89**, 222908 (2006).

¹⁷L. K. Chao, E. V. Colla, M. B. Weissman, and D. D. Viehland, *Phys. Rev. B* **72**, 134105 (2005).

¹⁸J. F. Scott, *J. Phys.: Condens. Matter* **18**, 7123 (2006).

¹⁹W. Kleemann, *J. Phys.: Condens. Matter* **18**, L523 (2006).